Materials Science-Poland, 39(3), 2021, pp. 446-457
http://www.materialsscience.pwr.wroc.pl/
DOI: 10.2478/msp-2021-0036

Influence of flame straightening on the properties of welded joints made of X2CrNi22-2 duplex steel

Artur Lange[1,*]

[1]Department of Metal Forming, Welding and Metrology, Faculty of Mechanical Engineering, Wrocław University of Science and Technology, Łukasiewicza 7/9 Street, 50-371 Wrocław, Poland

The study investigates the optimal conditions associated with flame straightening of welded joints in duplex steel grade X2CrNi22-2. The research aimed to assess the influence of heat, applied during flame straightening of welded structures in X2CrNi22-2 grade steel, on the properties of the welded joints. Based on the macroscopic, microscopic, and strength tests conducted on welding joints in X2CrNiN22-2-grade duplex steel that have been subjected to flame straightening, it was ascertained that post-welding flame straightening of this grade of steel, at a treatment temperature of 730°C, should not take place for >1 min. The temperature of 730°C has been chosen as a reference because of the assumption that the welded joints are heated to the temperature of 700–730°C during straightening with an acetylene-oxygen flame. The paper scrutinizes the questions of (i) what changes occur in the welded joints as a result of flame straightening carried out in this temperature range and (ii) what impact those changes have on the joint strength. The results of our study indicate that the duration of post-welding flame straightening of X2CrNiN22-2-grade duplex steel, at a treatment temperature of 730°C, should not exceed 1 min.

Keywords: *flame straightening, duplex steel, sigma phase*

1. Introduction

An important advantage of duplex steel in comparison with traditional austenitic steels is its lower content of expensive nickel and superior strength properties, in addition to its preservation of good deformability and corrosion resistance, including in environments containing chloride ions [1]. However, their limitation is their tendency for brittleness after annealing within the temperature range of 280–520°C (the so-called 475°C brittleness), which can appear after just several minutes of heat application, as well as sudden plasticity reduction caused by precipitation of the sigma and chi intermetallic phases, occurring within the temperature range of 610–950°C [2].

The mentioned adverse changes in ferritic and duplex steels also occur under the influence of welding heat. Therefore, it is justified to ask whether heating with an acetylene-oxygen flame during straightening of constructions made of these steels has a negative influence on the properties of welded joints, all the more so since the studied steel contains molybdenum.

With regard to flame straightening of constructions made of stainless steels, it is decidedly advisable not to apply such treatment for straightening of austenitic chromium-nickel steels [1]. However, there is no such indication with respect to ferritic and duplex steels. Moreover, analysis of the literature shows that flame straightening of duplex steels is practiced [3]. In Germany, training seminars on flame straightening of various constructions, including those made of duplex steel, are conducted [3]. Linde [4], a manufacturer of technical welding gases, also manufactures equipment for flame straightening, and its guidelines state that flame straightening of high-alloy austenitic steels generally leads to structural changes in addition to surface oxidation. However, the surface does not undergo change when the flame temperature is maintained between 550°C and 750°C (“dark red”) during straightening. Carburization is avoided with a neutral flame, and even with excess oxygen. Due to lower thermal conductivity and greater thermal expansion, heat accumulation and rapid action are

* E-mail: artur.lange@pwr.edu.pl

© 2021. This is an open access article distributed under the Creative Commons Attribution-NonCommercial-NoDerivatives 4.0 License. (http://creativecommons.org/licenses/by-nc-nd/4.0/)

achieved; and because of this, smaller torch nozzles are applied than in the case of structural steels. Rapid cooling has a beneficial influence on material quality and steel corrosion.

The possibility of subjecting duplex steel to flame straightening is assumed based on the following facts: (i) the grain growth observed in the high-temperature HAZ (Heat Affected Zone) zone (near the fusion line) occurs at high temperatures ($>$1,000°C), and such temperatures typically do not occur during straightening; and (ii) the process of intermetallic phase precipitation depends not only on temperature but also on heating time. It turns out that, for the linear energies applied during welding, the joint's cooling rate is greater than the critical rate of sigma phase formation [5]. As indicated in the chart presented in Xavier et al. [5] and as other studies have confirmed, the sigma phase should not precipitate.

However, the start and end times of the sigma phase precipitation process also depend on the chemical composition of the steel. A comparison of grade 2205 and 2507 duplex steels [6] shows that the sigma phase appears in 2205 grade steel after 1 h of heating at 800°C, while in grade 2507 steel, the sigma phase appears after just 6 min of heating at 700°C. Meanwhile, the process of chromium carbide and chromium nitride precipitation begins within a relatively short time of 1–2 min. The authors of the publications state that the kinetics of chromium carbide and chromium nitride precipitation for all duplex stainless steel alloys with nitrogen are similar to that for 2205 grade steel [6].

The most important intermetallic phases during production and welding of duplex steel are sigma, chi, secondary austenite, and chromium nitrides. All of these phases form at temperatures $>$500°C. When the temperature is $\leq$ 500°C, precipitation reactions are relatively slow, and thus the influence exerted on brittleness is small [7].

The literature shows that the fastest rate of sigma phase formation from ferrite takes place at a temperature of $\approx$ 750°C, and weld metals containing molybdenum exhibit the greatest tendency to form the sigma phase, followed by those containing silicon, tungsten, vanadium, and niobium, in order of decreasing intensity [8].

In order to limit heat efflux into the neighboring material (which should remain cool) and avoid inclusions of intermetallic phases (including the σ phase), the material should be heated within the shortest possible time [9]. The effect of annealing time on σ phase formation is addressed in the literature in a 1991 study [10], and also in a guide published by Linde [6].

Due to the risk of adverse effects occurring in the material during performance of the flame straightening process, this method is applied very rarely and only when necessary [11]. Duplex steel is used in the construction of means of transport, e.g., for vehicle frames. The large number of joining elements and welds promotes welding distortion in such structures. Flame straightening could be a cheap and quick way of straightening them. Further interesting conclusions that can be taken into consideration with regard to flame straightening of duplex steels are available in Łabanowski et al. [12]. The effect of heat treatments, including the resultant changes in microstructure and mechanical properties, mainly impact toughness, on duplex stainless steel and higher alloy superduplex steels is discussed in the study by Topolska and Łabanowski [13]. In their 2019 study [14], Golański and Lachowicz recognize the sigma phase present on ferrite grain boundaries as the reason for the brittle rupture of the suspension. An excellent description of the influence of heat on the presence of the sigma phase is available in the 2009 study by Garin and Mannheim [15]. The latest research confirms the possibility of testing with non-destructive techniques for the detection of the sigma phase in duplex stainless steel [16], which is difficult, however, because it requires appropriate preparation of the sample for testing. Moreover, despite the many available methods, the identification of the sigma phase in duplex steels is still a difficult issue [17]. It is true that sigma phase detection in duplex stainless steel is possible with an induced magnetic field [18]; however, it is rather difficult to detect the moment of its appearance in duplex steel when the sigma phase occurs in very small amounts.

2. Materials and methods

The subjects of the present research were (i) thermally untreated welded joints, which were designated by the letter S; and (ii) joints heated by flame to a temperature of 730°C, intended to simulate the heating occurring during flame straightening, which were designated by the letter W. The joints used were butt-welded joints having closed profiles of 30 × 30 mm, made of corrosion-resistant ferritic-austenitic steel of the grade X2CrNiN22-2. Figure 1 shows a view of the joints. Joints not subjected to heat treatment after welding were marked DS (Duplex Steel); and welded joints annealed after welding at 730°C were marked DSA (Duplex Steel Annealed). The joints were annealed for periods of 15 min, 5 min, 2.5 min, and 1 min, after which they were cooled in air. Samples were extracted from all joints for testing.

The scope of research included the following:

- Macroscopic observations of welded joints made with the unaided eye, and with a SMT-800 stereo microscope and a Neophot 32 light microscope at 20× magnification.
- Microscopic observations carried out with an OLYMPUS CK40M light microscope and registration of images taken with a CCD (Charge-Coupled Device) camera.
- Hardness measurements carried out using the Vickers method under the load of 9.807 N in conditions compliant with PN-EN ISO 6507:2007.
- Determination of weld strength properties according to PN-EN 10002 (2004) with the use of a VEB testing machine model FP2 100/1(Germany).

The tensile strength test of joints was performed on non-standard samples. Microscopic examinations of welded joints were conducted on cross-sections of welds in the native material, in the heat-affected zone near the fusion line and weld, and under magnifications ranging from 50× to 500×; the observation was carried out in the unetched state and then again after etching with Mi30Fe reagent according to the standard PN-H-04503:1961.

An OLYMPUS CK40M metallographic microscope, coupled with a CCD digital camera with image recording, was applied. Chemical composition analysis was performed in an argon atmosphere on a LECO GDS-750-QDP glow discharge spectrometer.

2.1. Chemical composition analysis

Samples for chemical composition studies were sourced from the 1.4062-grade duplex steel, and extracted from the weld. Figure 2 shows the samples used for the chemical composition analysis, and Table 1 shows the results of the analysis.

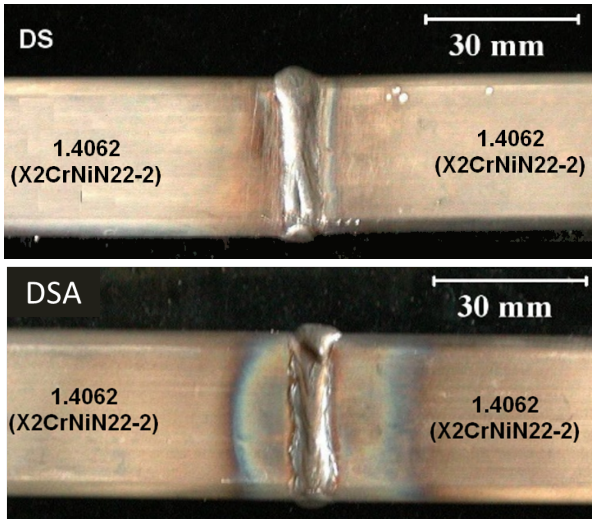


Fig. 1. General view of butt joint after welding (DS) and annealed joint after welding at 730°C (DSA)

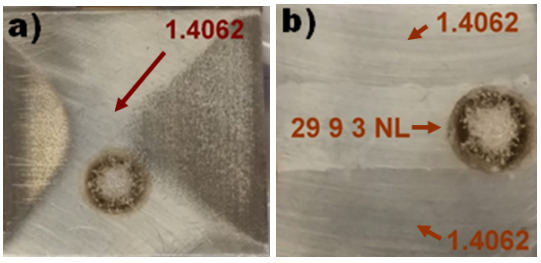


Fig. 2. View of duplex steel specimens of 1.4062 grade and wire welded joint EN ISO 14343-A: G 22 9 3 N L after analysis of chemical composition

Table 1. Results of the analysis of the chemical composition of tested materials

Cont.% by weight	**Steel grade 1.4062 (X2CrNi22-2)**		**Wire G 22 9 3 N L**	**Weld in the joint 1.4062+1.4062**
	Certificate No. 51513524	**Analysis results by LECO**	**Certificate No. 102004**	**Analysis results by LECO**
C	0.020	0.025	0.1	0.025
Si	0.450	0.30	0.5	0.41
Mn	1.340	1.33	1.7	1.68
P	0.023	0.030	0.016	0.030
S	0.001	0.015	0.001	0.013
Cr	22.800	22.05	22.9	22.60
Ni	2.640	2.46	8.8	7.68
Mo	0.210	0.19	3.1	1.86
Nb	–	0.03	–	0.03
Cu	–	0.23	<0.1	0.017
N	0.216	–	0.16	–
Co	–	0.05	–	0.06
V	–	–	–	0.07
W	–	–	–	0.01

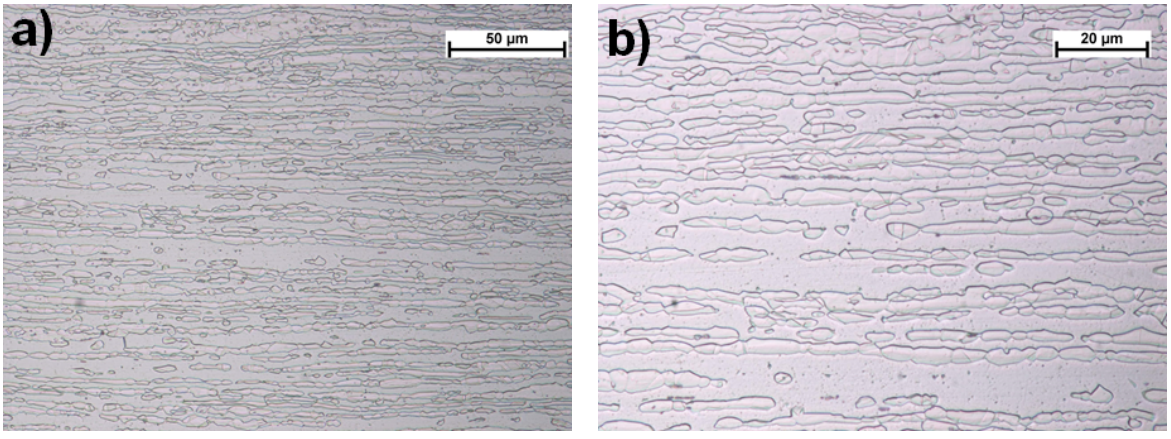


Fig. 3. Fine-grained ferritic-austenitic structure with diverse grain size and high intensity of banding. Light microscopy. Etched with Mi19Fe

Based on the results of the analysis of the chemical composition of the materials tested, it can be concluded that there was a low degree of mixing of the filler metal components with the steel components in the welded joints. This may be the result of shallow fusion of the weld metal into the joint parent material. The content of elements in a welded joint is very similar to the chemical composition of the alloy of the filler metal used.

2.2. Metallographic examinations

Microscopic examinations of native materials in the unetched state revealed a small amount of non-metallic inclusions, mainly in the form of oxides distributed in points.

After etching with Mi19Fe reagent, a fine-grained ferritic-austenitic structure with diverse grain size could be observed (Figure 3), with high intensity of banding, as typical for materials sub-

jected to metalworking (rolling).

The microscopic tests conducted in the vicinity of the fusion line of grade X2CrNiN22-2 duplex steel, in both butt welds S and W, revealed a ferritic-austenitic structure with expanded and recrystallized grains of ferrite and austenite, with visible σ phase clusters rich in Cr and Mo, forming in the area of ferrite grains and on the ferrite-austenite boundary (α/γ), as depicted in Figures 4–13. In the joint welded and soaked at 730°C (W), a rather substantial grain growth was observed, with a very large amount of intermetallic σ phase rich in chromium (Cr) and molybdenum (Mo). An aciform, dendritic, ferritic-austenitic structure was observed in welds, as depicted in Figures 14 and 15.

It should be mentioned that the sigma phase (σ) rich in Cr and Mo may precipitate in the

Structures after the welding process (S)

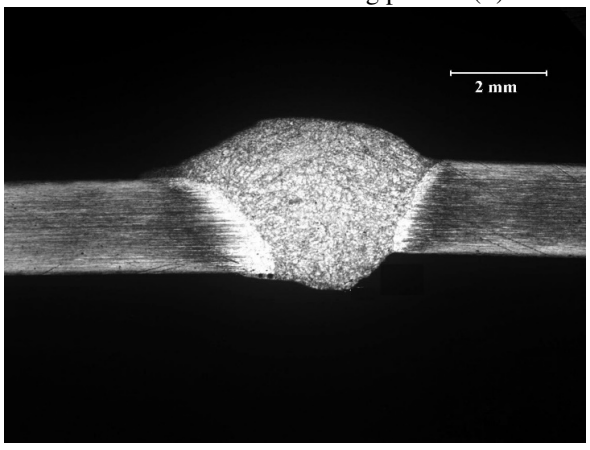


Fig. 4. Welded joint, S sample. Joint welded using duplex steel. Weld with ferritic-austenitic structure. Etched with Mi19Fe

Structures after the process of welding and soaking at 730°C (W)

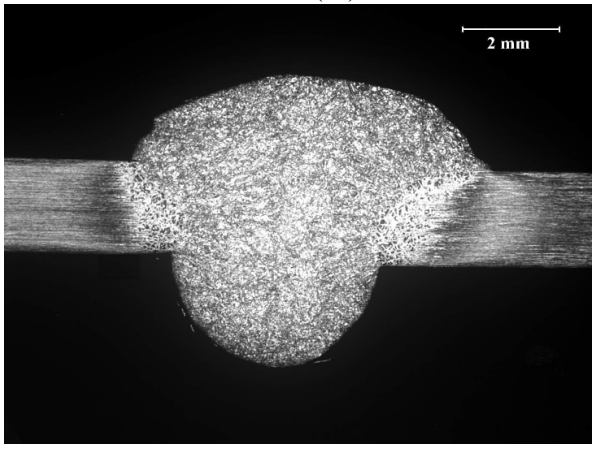


Fig. 5. Welded joint, W sample. Joint welded using duplex steel and soaked at 730°C. Weld with ferritic-austenitic structure. Etched with Mi19Fe

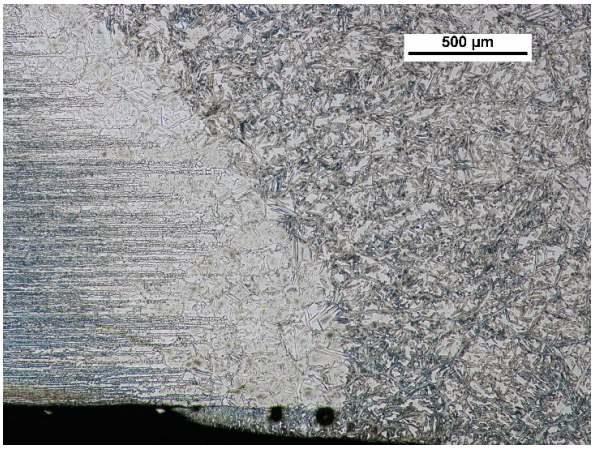


Fig. 6. Welded joint, S sample. Heat-affected zone in the vicinity of the fusion line from the side of the root. Visible ferritic-austenitic structure with expanded and recrystallized ferrite and austenite grains. Etched with Mi30Fe

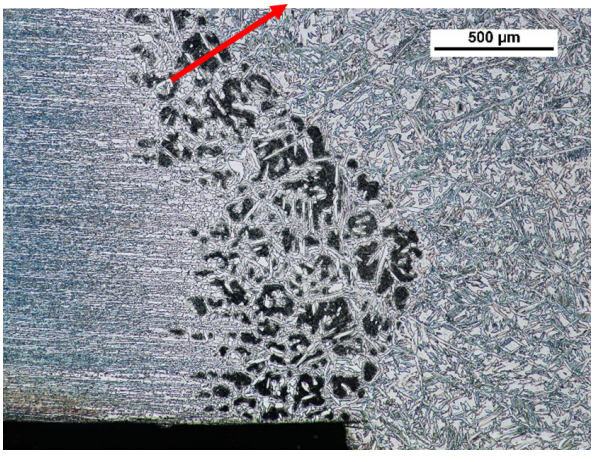


Fig. 7. Welded joint, W sample. Heat-affected zone in the vicinity of the fusion line from the side of the root. Visible ferritic-austenitic structure with expanded and recrystallized ferrite and austenite grains, and visible, numerous σ phase clusters rich in Cr and Mo, forming in the area of ferrite grains. Etched with Mi30Fe

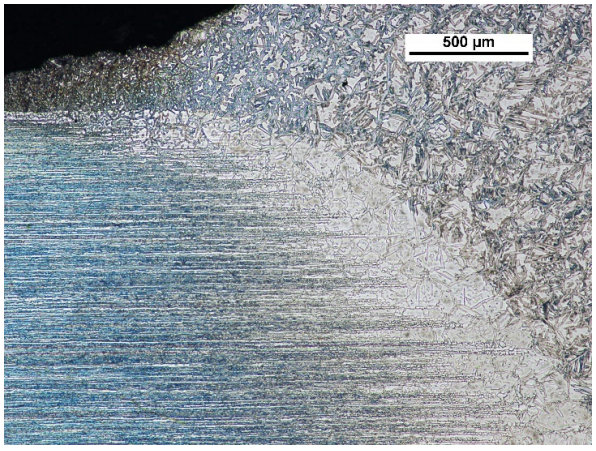


Fig. 8. Welded joint, S sample. Heat-affected zone. In vicinity of fusion line, from the side of the face, visible ferritic-austenitic structure with expanded and recrystallized ferrite and austenite grains. Etched with Mi30Fe

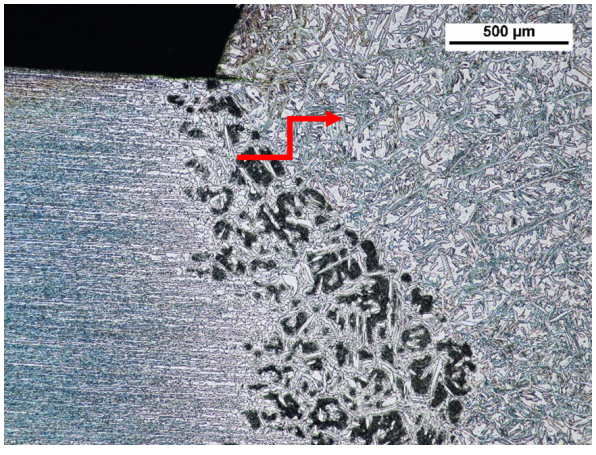


Fig. 9. Welded joint, W sample. Heat-affected zone in the vicinity of the fusion line from the side of the face. Visible ferritic-austenitic structure with expanded and recrystallized ferrite and austenite grains, and visible, numerous σ phase clusters rich in Cr and Mo, forming in the area of ferrite grains. Etched with Mi30Fe

650–1,000°C temperature change within the area of ferrite grains or on the ferrite-austenite boundary (α/γ) during the welding process, or may form as precipitations of secondary phases during heat treatment. This phase forms from ferrite, and causes depletion of adjacent areas of Cr and Mo, reduction in resistance to pitting and intercrystalline corrosion, and increase in brittleness. Elements such as chromium (Cr), molybdenum (Mo), manganese (Mn), silicon (Si), and tungsten (W)

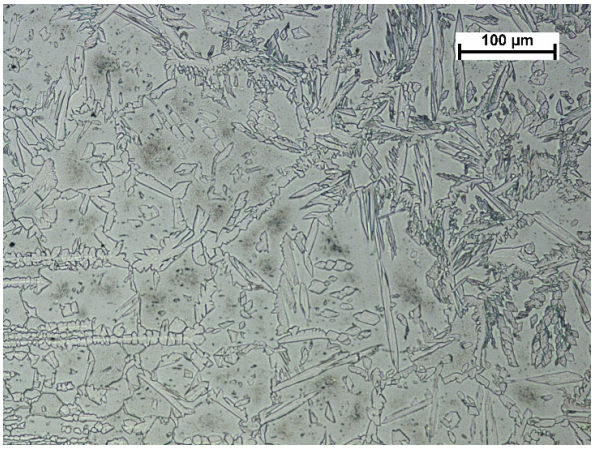


Fig. 10. Welded joint, S sample. Magnified fragment of the area shown in Figure 8. Heat-affected zone. In the vicinity of the fusion line, visible ferritic-austenitic structure with expanded and recrystallized ferrite and austenite grains, and visible, numerous σ phase clusters rich in Cr and Mo, forming in the area of ferrite grains. Etched with Mi30Fe

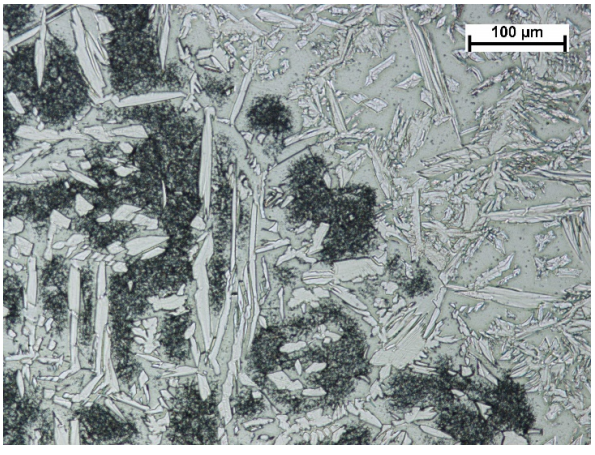


Fig. 11. Welded joint, W sample. Magnified fragment of the area shown in Figure 9. Heat-affected zone in the vicinity of the fusion line from the side of the root. Visible ferritic-austenitic structure with highly expanded and recrystallized ferrite and austenite grains, and visible, numerous σ phase clusters rich in Cr and Mo, forming in the area of ferrite grains. Etched with Mi30Fe

foster the formation of the σ phase [1].

Tests of the kinetics of sigma phase formation during soaking of type 18-8 weld metals at 750°C revealed that $\approx 70\%$ of delta ferrite degrades into the sigma phase and $\approx 30\%$ into secondary austenite, and this degradation typically begins after just 30 s [3].

The W welded joint was made with an excessively high face excess and large root leaks,

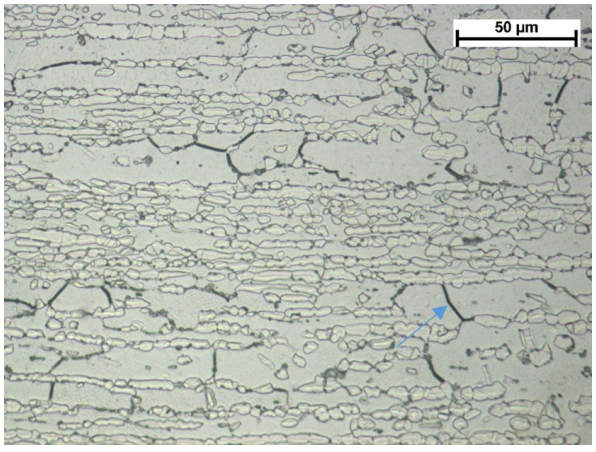


Fig. 12. Welded joint, S sample. Ferritic-austenitic structure with recrystallized ferrite and austenite grains, with visible precipitations of σ phase rich in Cr and Mo on the α/γ (ferrite-austenite) boundary. Etched with Mi19Fe

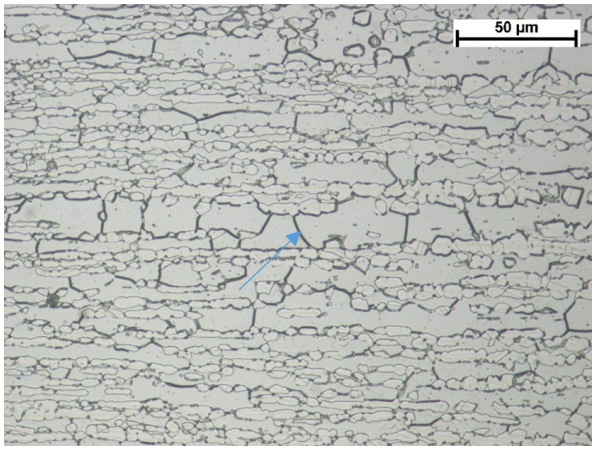


Fig. 13. Welded joint, W sample. Ferritic-austenitic structure with recrystallized ferrite and austenite grains, with visible precipitations of σ phase rich in Cr and Mo on the α/γ (ferrite-austenite) boundary. Etched with Mi19Fe

which indicates a large supply of heat. Thus, it was not possible to precisely determine whether sigma phase precipitations formed as a result of the welding process or the additional heat treatment, which is why it was decided to soak the other parts of S samples at 730°C for 15 min, 5 min, 2.5 min, and 1 min in a silit rod furnace without a protective atmosphere, with cooling in air, and to conduct additional microscopic observations.

The conducted microscopic examinations revealed that in the DS and TS samples, in the heat-affected zone in the X2CrNiN22-2-grade duplex-steel material (designated No. 1.4062), during

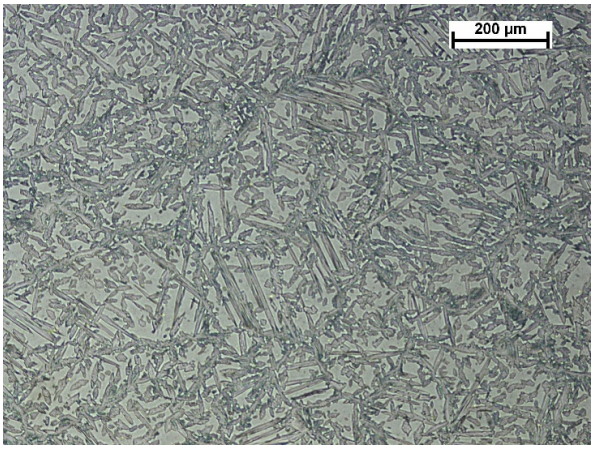


Fig. 14. Welded joint, S sample. Weld. Visible dendritic, aciform, ferritic-austenitic structure. Etched with Mi30Fe

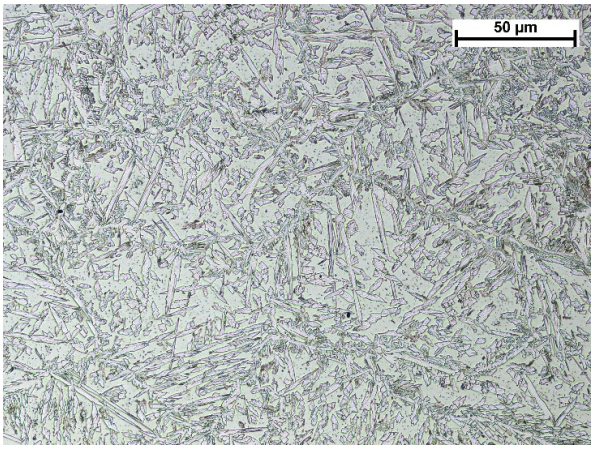


Fig. 15. Welded joint, W sample. Weld. Visible dendritic, aciform, ferritic-austenitic structure. Etched with Mi30Fe

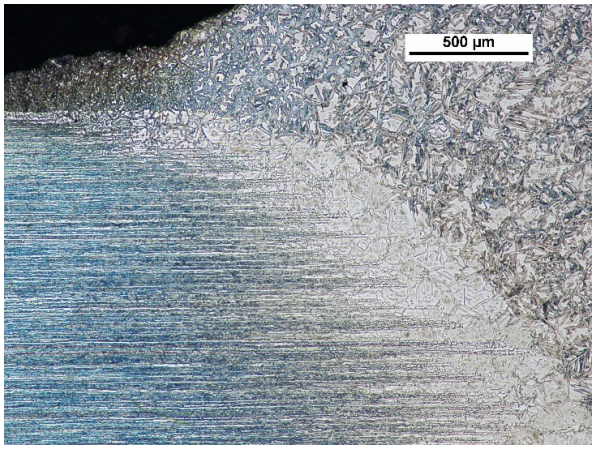


Fig. 16. Welded joints, S sample prior to soaking in furnace at 730°C. Heat-affected zone. In vicinity of fusion line, from the side of the face, visible ferritic-austenitic structure with recrystallized ferrite and austenite grains. Etched with Mi30Fe

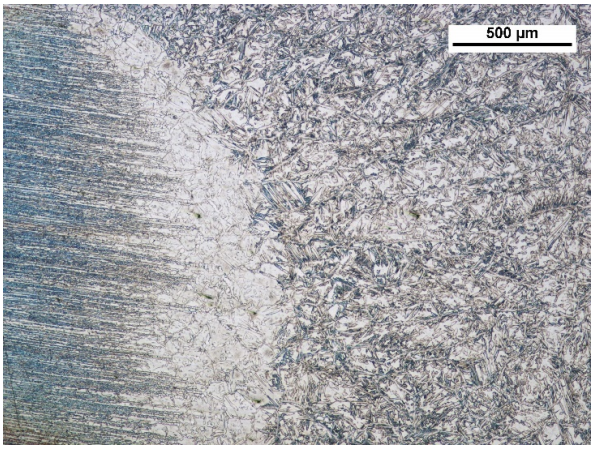


Fig. 18. Welded joints, S sample prior to soaking in furnace at 730°C. Heat-affected zone. In vicinity of fusion line, from the side of the face, visible coarse-grained ferritic-austenitic structure with recrystallized ferrite and austenite grains. Etched with Mi30Fe

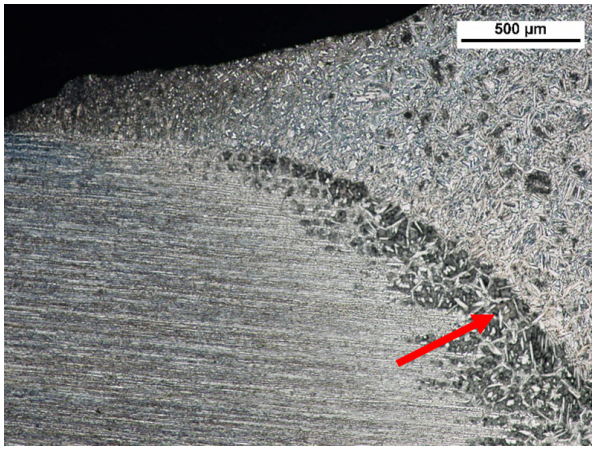


Fig. 17. Welded joint, S sample. Soaked in silit rod furnace at 730°C for 15 min and cooled in air. Heat-affected zone in the vicinity of the fusion line from the side of the face. Visible ferritic-austenitic structure with recrystallized ferrite and austenite grains, and visible, numerous σ phase clusters rich in Cr and Mo, forming in the area of ferrite grains. Etched with Mi30Fe

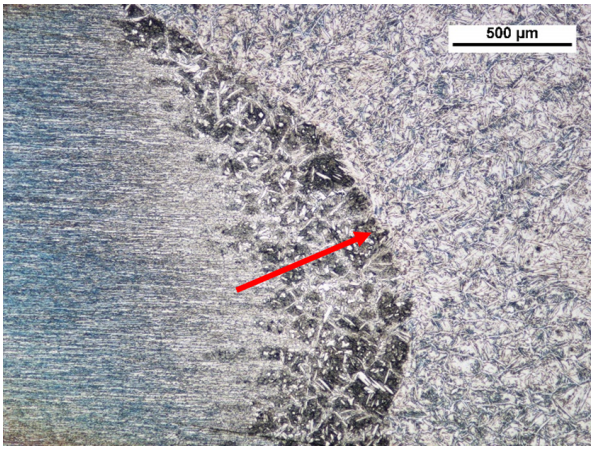


Fig. 19. Welded joint, S sample. Soaked in silit rod furnace at 730°C for 5 min and cooled in air. Heat-affected zone in the vicinity of the fusion line from the side of the face. Visible coarse-grained ferritic-austenitic structure with recrystallized ferrite and austenite grains, and visible, numerous sigma (σ) phase clusters rich in Cr and Mo, forming in the area of ferrite grains. Etched with Mi30Fe

soaking at 730°C over the course of 15 min, 5 min, and 2.5 min, and cooling in air, a greater amount of sigma (σ) phase precipitated in ferrite and on the ferrite-austenite (α/γ) boundary than in the same sample prior to the soaking process (Figures 16–19); and in the sample soaked at 730°C for 1 min and cooled in air, no sigma (σ) phase precipitations were identified in ferrite or on the ferrite-austenite (α/γ) boundary (Figure 20).

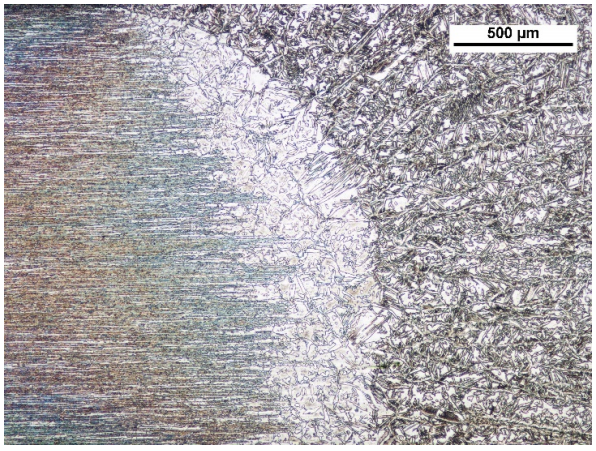


Fig. 20. Welded joint, S sample. Soaked in silit rod furnace at 730°C for 1 min and cooled in air. Heat-affected zone. In vicinity of fusion line, from the side of the face, visible coarse-grained ferritic-austenitic structure with recrystallized ferrite and austenite grains. No sigma (σ) phase precipitations rich in Cr and Mo were identified. Etched with Mi30Fe

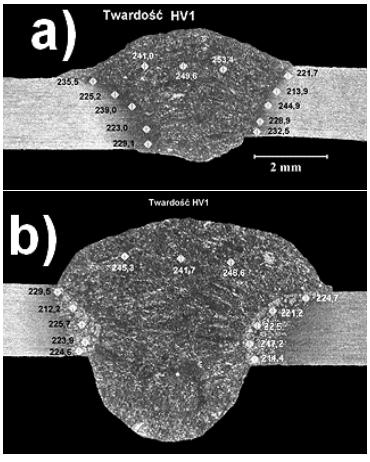


Fig. 21. System of hardness measurement points in heat-affected zones and weld: **(A)** welds without heat treatment after welding, S sample, **(B)** joints heated by acetylene-oxygen flame to ≈ 730°C, W sample

2.3. Hardness measurements

Hardness measurements of welded joints were performed using the Vickers method, according to PN-EN ISO 650: 2007. A Zwick 321 hardness tester was applied with the penetrator under a load of 9.807 N, acting for a time of 15 s. The system

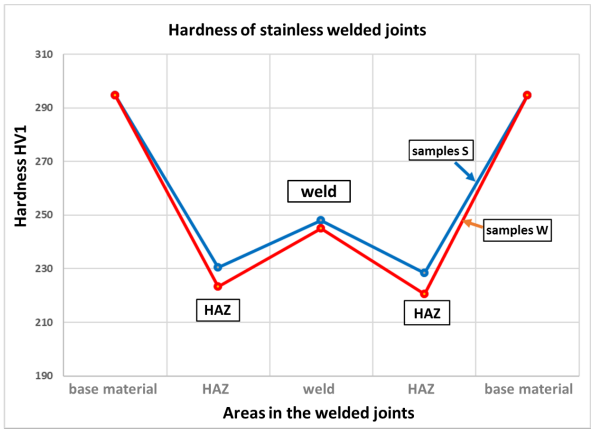


Fig. 22. HV1 hardness distribution in joints without heat treatment after welding (S samples), **b)** joints heated by acetylene-oxygen flame to ≈ 730°C (W samples)

of hardness measurement points on the metallographic specimen of the joint is shown in Figure 21.

The hardness of the native material, duplex steel, was 295 HV1, the hardness of the joint without heat treatment after welding in the heat-affected zone near the fusion line was 229 HV1, and the hardness of the joint was 248 HV1; further, the hardness of the joint heated with a flame to ≈ 730°C amounted to 222 HV1 and 245 HV1 in the HAZ and in the weld, respectively. Hardness change in the tested joints is presented in Figure 22.

The decrease in hardness in the heat-affected zone is mainly the result of recrystallization of the material's structure, which was in a state of cold work after rolling. The results of the conducted hardness measurements indicated that the process of soaking the welded joints at 730°C in the HAZ near the fusion line did not cause significant differences in hardness. The small hardness reduction visible in Figure 22 results from further recrystallization of the material's structure during soaking.

2.4. Tensile strength evaluation

Three flat specimens in the form of strips were collected according to PN-EN ISO 6892-1, Appendix E, for tests from every sample group. The results of strength tests are shown in Table 2, and the appearance of specimens after the tensile test is shown in Figure 23.

Table 2. Results of static tensile test of specimens of butt welds without heat treatment after welding (S samples) and butt welds heated with acetylene-oxygen flame to ≈ 730°C (W samples)

Item no.	Designation of joint specimen	a×b (mm)	S_0 (mm^2)	F_m (N)	R_m (MPa)	R_m avg (MPa)	R_m (MPa) according to PN-EN 10088-2
1.	Sb	19.94 × 1.98	39.5	2,6600	**673***		
2.	Sc	19.94 × 1.94	38.6	28,400	**736**	**727**	
3.	Sd	19.94 × 1.96	39.1	30,200	**772**		**700–900**
4.	Wb	19.95 × 1.91	38.1	27,200	**714**		
5.	Wc	19.8 × 1.89	37.4	29,400	**786**	**739**	
6.	Wd	19.86 × 1.91	37.9	27,200	**718**		

*Welding non-conformity occurring in weld (partial lack of melting).

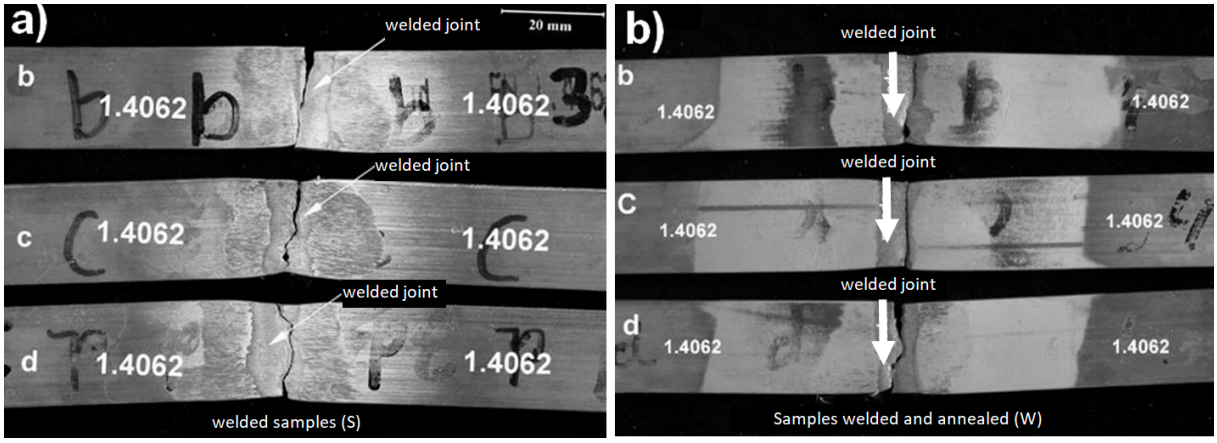


Fig. 23. General view of specimens of butt-welded joints after tensile test: **(A)** welds without heat treatment after welding, S samples, **(B)** joints heated by acetylene-oxygen flame to ≈ 730°C, W samples. Fracture in weld

Based on the performed strength tests of butt-welded joints without heat treatment after welding and joints heated by acetylene-oxygen flame to ≈ 730°C, it was determined that fracture in the specimens occurred in the weld.

The tested joints were made with one bead, which resulted in a low tendency for sigma-phase precipitation in the HAZ near the fusion line and in the weld. The appearance of the sigma phase in such a configuration does not have a significant influence on the strength of welded joints. Even the appearance of a small amount of sigma phase in root layers of multi-layered welds does not significantly reduce the strength and plasticity properties of welded joints made of type 18-8 steel [3].

3. Conclusions

1. Microscopic examinations of the native material, duplex steel, in the unetched state, showed that there is a small amount of non-metallic inclusions distributed uniformly in points, mainly in the form of oxides. After etching with Mi30Fe reagent, it was determined that the steel has a fine-grained ferritic-austenitic structure with diverse grain size, with high intensity of banding, as typical for materials subjected to metalworking (rolling).
2. The conducted microscopic examinations of the welded joints revealed that a ferritic-austenitic structure with expanded and re-

crystallized ferrite and austenite grains is present in the vicinity of the fusion line. In the joint welded and heated with flame to $\approx 730^{\circ}$C, much larger grain growth was observed in comparison with joints without heat treatment, with visible σ-phase clusters rich in Cr and Mo forming in the area of ferrite grains and on the ferrite-austenite (α/γ) boundary. An aciform, dendritic, ferritic-austenitic structure was observed in welds.

3. In the sample soaked at 730°C for 1 min and then cooled in air, no sigma (σ) phase precipitations were identified in ferrite and on the ferrite-austenite (α/γ) boundary, while in samples soaked at 730°C for 15 min, 5 min, and 2.5 min and then cooled in air, the amount of the sigma (σ) phase in ferrite and on the ferrite-austenite boundary increased as soaking time increased.
4. The conducted hardness measurements revealed that the process of soaking the welded joints at 730°C did not cause significant differences in hardness in the HAZ near the fusion line. The mean hardness of the native material, duplex steel, was 295 HV1, the hardness of the joint without heat treatment after welding in the heat-affected zone near the fusion line was 229 HV1, and the hardness of the joint was 248 HV1; further, the hardness of the joint heated with a flame to $\approx 730^{\circ}$C amounted to 222 HV1 and 245 HV1 in the HAZ and in the weld, respectively.
5. The tensile strength of butt-welded joints amounted to 727 MPa without heat treatment and 739 MPa after annealing. During the tensile test of duplex steel butt-welded joints, the fracture always occurred in the weld, regardless of whether heat treatment was applied after welding. This is rather atypical behavior, since fracturing of welded joints in the weld material generally indicated inadequate filler metal or improper welding technology.
6. Based on the macroscopic, microscopic, and strength tests conducted on welding joints in X2CrNiN22-2-grade duplex steel that have been subjected to flame straightening, it was ascertained that post-welding flame straightening of this grade of steel, at a treatment temperature of 730°C, should not take place for >1 min. Hence, when flame straightening constructions made of this steel, temperature and heating time must be controlled precisely.

References

[1] Tasak E, Ziewiec A. Spawalność materiałów konstrukcyjnych. Kraków: Wydawnictwo JAK; 2009.

[2] Nowacki J. Spawalność stali dupleks. Przegląd Spawalnictwa. 2008;10:34–44.

[3] Dienstleitungen und Veranstaltungen. GSI-SLV Muenchen; 2016.

[4] Expertenwissen: Flammrichten (online access: `https://docplayer.org/113108652-Expertenwissen-flammstrahlen-flammstrahlen-flammrichten-lichtbogen-handschweissen-duplex-stahl-plasmaschneiden.html`, 14.12.2021).

[5] Xavier CR, Delgado HG Jr, de Castro JA. An experimental and numerical approach for the welding effects on the Duplex stainless steel microstructure. Mater Res. 2015;18(3):489–502. (doi.org/10.1590/1516-1439.302014)

[6] BOC. Fundamentals of flame straightening, Technical information for flame processes. Catalog available at: `https://www.boconline.co.uk/en/images/Fundamentals-of-Flame-Straightening_tcm410-113398.pdf`. Accessed 15 May 2019.

[7] Topolska S, Łabanowski J. Impact-toughness investigations of duplex stainless steels. Materiali in tehnologije/Mater Technol. 2015;49(4):481–6.

[8] Klimpel A. Wpływ pierwiastków stopowych na tworzenie się fazy sigma w stopiwach austenityczno-ferrytycznych typu 18-8. Zeszyty naukowe Politechniki Śląskiej, No. 509.

[9] Słania J. Elimination of welding distortions. Przegląd Spawalnictwa/Welding Technology Review p. 36-40, 2012;2.

[10] Ch. Bohlen. Flammrichten von Duplexstahl X2 CrNiMoN2253, Der Praktiker. Schweißen und Schneiden 1991;43(1):4–5.

[11] van Nassau L, Meelker H, Neessen F, Hilkes J. Welding duplex and superduplex stainless steel, An update of the guide for industry.(access online: `https://www.google.com/url?sa=t&rct=j&q=&esrc=s&source=web&cd=&ved=2ahUKEwj21qKhkOP0AhVho4sKHfdHA44QFnoECAgQAQ&url=http%3A%2F%2Flasgroepregionoord.be%2Fwordpress%2Fwp-content%2Fuploads%2F2017%2F07%2F003-Update-guide-Welding-duplex-and-superduplex-stainless-steel.pdf&usg=AOvVaw1DXWs1sBtr8up25tY32H5q`)

[12] Łabanowski J, Świerczyńska A, Topolska S. Effect of microstructure on mechanical properties and corrosion resistance of 2205 duplex stainless steel. Pol Marit Res. 2014;21(4(84)):108–12. (doi.org/10.2478/pomr-2014-0047)

[13] Topolska S, Łabanowski J. Effect of microstructure on impact toughness of duplex and superduplex stainless steels. J Achiev Mater Manuf Eng. 2009;36(2):142–9.

[14] Golański G, Lachowicz MM. Failure cause analysis for the suspension element of boiler superheater. Eng Fail Anal. 2019;105:490–5. (10.1016/j.engfailanal.2019.07.024)

[15] Garin JL, Mannheim RL. Sigma-phase precipitation upon industrial-like heating of cast heat-resistant steels. J Mater Process Technol. 2009;209:3143–8. (doi.org/10.1016/j.jmatprotec.2008.07.026)

[16] Biezma MV, Martin U, Linhardt P, Ress J, RodrĂguez C, Bastidas MD. Non-destructive techniques for the detection of sigma phase in duplex stainless steel: a comprehensive review. Eng Fail Anal. 2021;122. p.1-36. (doi.org/10.1016/j.engfailanal.2021.105227)

[17] Llorca-Isern N, López-Luque H, López-Jiménez I, Biezma MV. Identification of sigma and chi phases in duplex stainless steels. Mater Charact. 2016;112, p. 20-29.. (doi.org/10.1016/j.matchar.2015.12.004)

[18] Silva EM, Fialho WML, Silva HFBM, Leite JP, Oliveira AVG. Sigma phase detection in duplex stainless steel by induced magnetic field. J Phys Conf Ser. 2015;733, p. 1-6 (doi.org/10.1088/1742-6596/733/1/012070)

Received 2021-10-27
Accepted 2021-12-04